# Exploring the material removal mechanism of 4H-SiC based on ultrasonic-assisted single-asperity scratching

**Ximin Ye[1], Hanqiang Wu[1], Chen Xiao[2] and Yongbo Wu[1,#]**
1 Department of Mechanical and Energy Engineering, Southern University of Science and Technology, Shenzhen 518055, China
2 Research Institute of Frontier Science, Southwest Jiaotong University, Chengdu 610031, China
# Corresponding Author / Email: wuyb@sustech.edu.cn, TEL: +86-18710242998

KEYWORDS: Ultrasonic assisted single-asperity scratching, 4H-SiC, material removal mechanism

*Ultrasonic-assisted polishing（UAP）of silicon carbide（SiC）wafers can effectively improve processing efficiency and wafer surface quality, making it widely applied in the SiC semiconductor manufacturing industry. However, the potential of UAP has not been sufficiently developed because the mechanism of interaction between the single abrasive particle and the wafer surface is so far elusive. In this study, the single-asperity material removal behaviors of single crystal 4H-SiC against the diamond AFM tip were quantitatively investigated with respect to the normal load under the presence and absence of ultrasonic vibration. The experimental results showed that the ultrasonic vibration slightly enhanced the material removal rate in the low normal load regime and obviously in the high normal load regime, with the friction force only decreasing in low and medium normal loads during single-asperity scratching. After concluding, specific friction and material removal explanations were proposed to clarify the interaction mechanism between the diamond tip and the SiC surface. The results would promote understanding the material removal mechanism in the ultrasonic-assisted polishing of SiC wafers.*

## 1. Introduction

Single crystal silicon carbide (SiC) possesses excellent material properties such as high hardness, high thermal conductivity, high temperature and corrosion resistance. As a result, it is widely used in fields such as semiconductors, optoelectronics, and wear-resistant materials, including power electronic devices and abrasive tools. [1,2] The crystal structure of 4H-SiC is a zinc blende structure, which has high strength and good chemical stability, making it one of the most promising wide-bandgap semiconductor materials for the future. However, its surface quality directly affects the performance and lifespan of devices, as surfaces with high roughness can lead to electric field concentration, breakdown, and other failure phenomena, compromising the stability and longevity of components. [3] Therefore, an appropriate processing method must be selected to achieve high surface quality and efficient processing of 4H-SiC.

Polishing is essential to improve the surface quality of hard-to-machine materials like SiC. In traditional polishing processes, the high hardness of silicon carbide often leads to severe wear on the polishing wheel, generating large friction forces, and its brittle nature can easily cause defects such as cracks, which negatively impact surface quality and processing efficiency. Neslen et al. [4] conducted SiC polishing experiments to investigate the effects of different polishing parameters on surface roughness, revealing that friction forces are closely related to the material removal rate, and excessive friction forces can deteriorate surface quality. Additionally, Luo et al. [5] studied the polishing process and proposed strategies to optimize friction forces, showing that the appropriate size of bonded abrasive particles and polishing parameters can significantly improve surface quality and extend the lifespan of the polishing wheel.

Ultrasonic-assisted polishing technology is a compound processing method that superimposes ultrasonic vibration onto the material removal behaviors. Compared to traditional polishing, it offers advantages such as lower friction forces, lower polishing temperatures, and longer polishing wheel lifespans. [6] It has been proven to be an effective solution for processing hard materials. Chen et al. [7] and Ban et al. [8] conducted ultrasonic-assisted polishing experiments and

simulations on SiC, showing that ultrasonic vibration reduced normal and friction forces, respectively. Zhao et al. [6] investigated polishing wheel wear during ultrasonic-assisted polishing of SiC, concluding that introducing ultrasonic vibration reduced the polishing wear coefficient by up to 40%. However, no published reports have completely explained material removal behavior in the SiC ultrasonic-assisted polishing process.

## 2. Theoretical Background of Material Removal Mechanism

It is widely acknowledged that single-asperity material removal behavior is highly complex due to the influence of numerous uncontrolled factors. In many single-asperity contact systems, material removal may result from the simultaneous action of multiple mechanisms, making it difficult to accurately predict the characteristics of the process [9]. Over the years, various models have been developed to estimate material removal depth and volume, with Archard's wear equation being the most broadly applicable [10]. The equation is expressed as:

$$V = \frac{K'' F_n L}{H} \tag{1}$$

Where $V$ is the material removal volume, $K''$ is the material removal volume coefficient, $H$ is the hardness of the substrate, $F_n$ is the applied normal load, and $L$ is the total scratching distance.

To verify the applicability of this equation at the nano-scale, researchers compared experimental test results at the nano-scale with those predicted by Archard's wear equation [11,12]. These studies revealed that, in contrast to macro-scale material removal behavior, the material removal volume of micro- and nano-scale components does not necessarily vary proportionally with applied load or inversely with specimen hardness. Consequently, the revised Archard's wear equation [13] is deemed more appropriate for use at the micro- and nano-scale levels

$$V = K' F_n^{x'} L^{y'} \tag{2}$$

where $x'$ and $y'$ are sensitive exponents, which are determined using data from the different experimental systems. For single-asperity scratching, the material removal depth, $h$, increases with the material removal volume, $V$, where $V$ is usually proportional to $h^2$ while the damaged trace shows a similar triangular shape. Thus, Eq. (2) can be rewritten as:

$$h = K'^{\frac{1}{2}} F_n^{\frac{x'}{2}} L^{\frac{y'}{2}} = K F_n^x L^y \tag{3}$$

where $K$ is the new material removal depth coefficient, and the sensitive exponents $x$ and $y$ represent the material removal response. Higher values of $x$ or $y$ indicate that load and cycles influence material removal depth more significantly.

## 3. Material and Methods

### 3.1 Material Used in the Investigation

The single-asperity scratching tests were conducted on the Si surface of a two-side polished silicon carbide (SiC) wafer with a wafer size of 5×5×0.35 $mm^3$ (Hefei Crystal&Surface Technical Material Co., Ltd., China). The type/dopant of this SiC is 4H-N with the orientation 4.0 degrees off the (0 0 0 1) axis. Young's modulus, $E$, and hardness, $H$, of the 4H-SiC were determined as 413 GPa and 36 GPa, respectively [14]. With atomic force microscopy (AFM, Dimension Edge, Germany), the root-mean-square (RMS) roughness of the Si surface was measured under 0.5 nm over a 3×3 $\mu m^2$ area. A diamond tip (NC-LC, Adama Innovations, Ireland) was used to perform all the single-asperity scratching tests under the presence and absence of ultrasonic vibration. It has a curvature radius, $R$, of 20 nm and a nominal spring constant, $K$, of 100 N/m.

### 3.2 Force Calibration of AFM

For a commercial AFM, both the bending and torsion of the probe cantilever can be measured simultaneously by tracking the laser beam's lateral and vertical deflections while scanning the sample in the $x$–$y$ plane. The feedback from the vertical deflection represents the normal force, while the lateral deflection corresponds to the friction force [15]. Since these deflections are captured using a four-quadrant photodiode, the measured normal and friction forces are initially recorded as voltage signals. To quantitatively analyze material removal behavior with accurate normal force, it is essential to convert voltage signals of normal load into force values through force calibration. Based on information from the Burker website, the applied normal load can be determined using the equation:

$$F = KSI \tag{4}$$

where $K$ is the spring constant of the probe cantilever, $S$ is the sensitivity coefficient of the diamond tip measured by AFM, and $I$ is the voltage signal.

In contrast, for friction force analysis, the focus is on comparing the relative effects of ultrasonic vibration under different normal loads

rather than the precise force values. Therefore, while converting the voltage signals to force is essential for the normal force, the exact numerical values for friction force are less critical in this context.

### 3.3 Material Remove Experiments

All single-asperity scratching tests were conducted using an AFM (Dimension Edge, Germany) in ambient air with relative humidity between 50% and 60%. The ultrasonic vibration parameters were fixed at an amplitude of 10 nm and a frequency of 55 kHz, with the vibration direction perpendicular to the scratching direction. In the different scratching tests, the applied normal load ($F_n$) between the diamond tip and the SiC surface was adjusted from 4 to 64 μN, with a scratching time of 50 seconds and a scratching speed of 2 μm/s. During each test, the friction voltage signals were recorded, and the friction force in voltage form was calculated by taking half of the absolute difference between the two nearly parallel voltage signals on the friction signal plots. After the tests, the material removal areas were scanned in tapping mode using a sensitive silicon tip with a radius of curvature of 7 nm and a nominal spring constant of 26 N/m (OTESPA-R3, Bruker, Germany). The average material removal depths and volumes were then measured from the cross-sectional profiles of the scratches.

## 4. Results and Discussion

After scanning the material removal areas with a sensitive silicon tip, the scratches' topography with and without the ultrasonic vibration was obtained, as shown in Figs. 2 and 3. For $F_n$ below 16 μN, the difference in average material removal depth and volume between traditional scratching and ultrasonic-assisted scratching was minimal. However, when $F_n$ was in the range of 24 μN to 48 μN, the effect of ultrasonic vibration on the material removal depth and volume was gradually significant. Notably, as $F_n$ increased from 56 μN to 64 μN, the scratches' depth and volume increased sharply with the assistance of the ultrasonic vibration compared with those obtained under the traditional scratching. To quantify the impact of ultrasonic vibration under different normal loads on the material removal behavior of 4H-SiC, the average material removal depth and volume as a function of $F_n$ is plotted in Fig. 4. The following discussion provides potential explanations for the observed variation in ultrasonic vibration's effectiveness with increasing normal load.

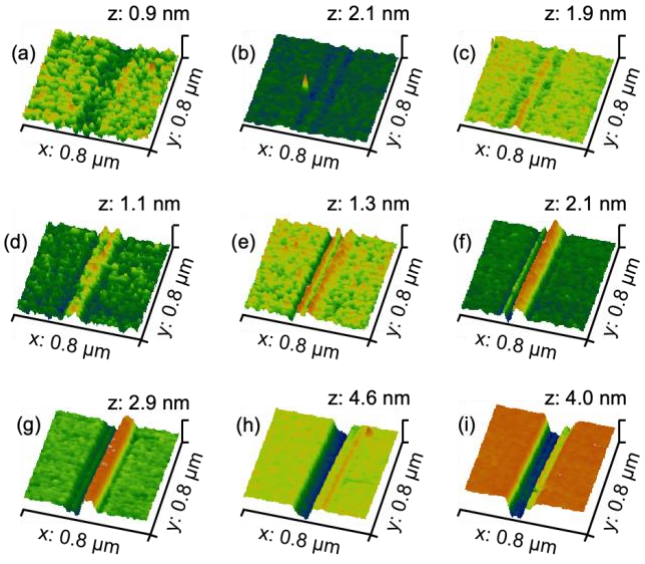


Fig. 2 The AFM topography images under different normal loads of (a)4, (b)8, (c)16, (d)24, (e)32, (f)40, (g)48, (h)56 and (i)64 μN with scratching speed of 2 μm/s, scratching time of 50 s and no ultrasonic vibration.

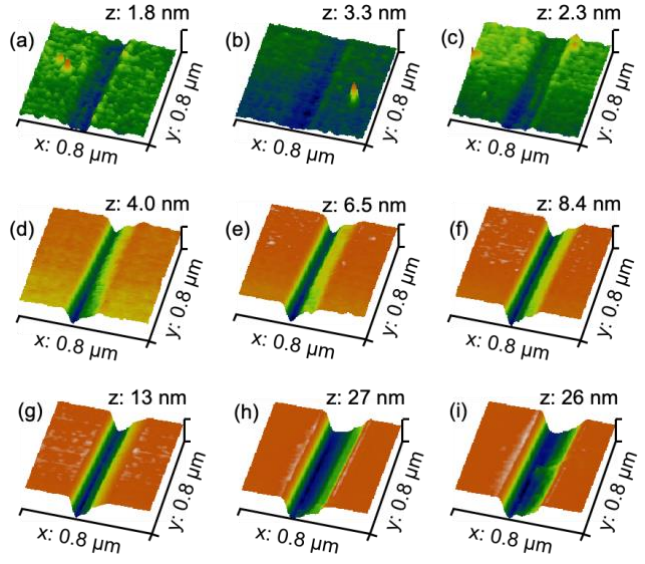


Fig. 3 The AFM topography images under different normal loads of (a)4, (b)8, (c)16, (d)24, (e)32, (f)40, (g)48, (h)56 and (i)64 μN with scratching speed of 2 μm/s, scratching time of 50 s and ultrason ic vibration.

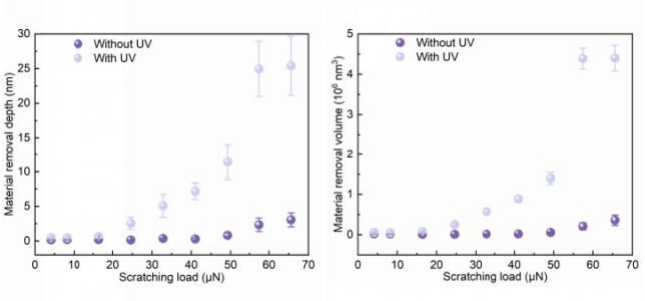


Fig. 4 Material removal depth and volume under different scratching loads with and without the ultrasonic vibration.

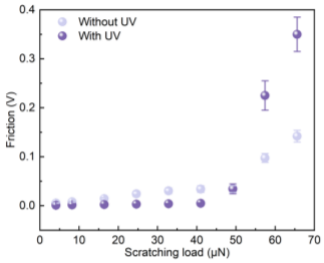


Fig. 5 Average friction force in voltage form under different scratching loads with and without the ultrasonic vibration.

In the low normal load region ($F_n \leq 16$ μN), no significant damage was observed in the absence of ultrasonic vibration, indicating that elastic deformation dominated the scratching process. As $F_n$ increased, visible grooves and material pile-up along the sides of the grooves began to appear. The material removal depth and volume were found to increase nonlinearly with $F_n$, showing a slight rise in the low load regime ($F_n \leq 16$ μN) and a sharp increase in the higher load regime ($F_n \geq 16$ μN).

Plastic deformation occurs when the mean contact pressure, $P$, exceeds $1.1Y$, where $Y$ is the material's yield stress [16]. Once plastic deformation begins, the scratching motion of the tip induces friction force of plowing, leading to visible wear traces. The mean contact pressure, $P$, for a conical diamond tip in contact with the substrate can be estimated using the following equation [17]:

$$P = \frac{2}{3\pi}\left(\frac{6F_n E^{*2}}{R^2}\right)^{\frac{1}{3}} \quad (5)$$

The material yield stress, $Y$, can be estimated using the Bowden and Tabor relation [18], $Y=H/3$, where H is the hardness of the material, which is 36 GPa for the SiC. Accordingly, the yield stress Y of SiC is approximately 12 GPa. For $F_n$=16 μN, $P$ was calculated to be lower than $1.1Y$. Therefore, the contact between the tip and the SiC can be considered elastic, resulting in no visible scratching trace on the SiC surface. Once the normal load exceeded 16 μN, the contact transitioned to an elastic-plastic regime, and friction force of plowing began to occur. When $F_n$ was between 24 and 48 μN, the corresponding contact pressures $P$ were just a little bit larger than the yield stress of SiC. As a result, plastic deformation remained relatively slight, with elastic deformation playing a more dominant role under these load conditions, causing only a slight increase in material removal depth and volume. As the load continued to increase, plastic deformation became more pronounced, leading to significant wear or material removal under higher loads. Consequently, the material removal depth and volume increased sharply in the high-load regime. These findings align with the friction data presented in Fig. 5, which indicated that the friction force of plowing when $F_n \leq 48$ μN is lower than the friction force of wear when $F_n \geq 48$ μN.

Under the presence of ultrasonic vibration, as illustrated in Fig. 3, material removal was observed at all normal load levels during single-asperity scratching. As the normal load increased, the cross-sectional area of the material removal region became wider and deeper. Furthermore, it was found that ultrasonic vibration slightly enhanced the material removal rate in the low normal load regime and significantly in the high normal load regime, as shown in Fig. 4. Interestingly, Fig. 5 revealed that, compared to the traditional scratching, the friction force decreased only in the low to medium normal load ranges when ultrasonic vibration was applied. Experimental data showed that in the normal load range of 24 to 48 μN, ultrasonic vibration significantly increased the material removal depth and volume, even while reducing or maintaining frictional force. This result was particularly exciting, as it suggested that this specific range of parameters can greatly enhance processing efficiency in the industry.

We attributed this phenomenon to the following: when the normal load is below 24 μN, the contact mode between the tip and the SiC remained predominantly elastic. In this regime, the elastic deformation of the material is not significantly influenced by the increased speed and distance brought by ultrasonic vibration. However, in the normal load range of 24 to 48 μN, plastic deformation became more pronounced, although elastic deformation still played an important role. In this load range, the increased speed and scratching distance induced by ultrasonic vibration affected the amount of plastic deformation and even led to wear or material removal, resulting in a notable increase in material removal depth and volume. At the same time, the presence of elastic deformation and the significantly higher relative speed due to ultrasonic vibration served to reduce the friction force acting on the single-asperity. When the normal load exceeded 48 μN, the contact mode shifted with no elastic contribution. In this regime, material removal dominated, and the friction force became directly proportional to the normal load, while the material removal depth and volume were influenced only by the increased scratching distance. Consequently, it was observed that ultrasonic vibration significantly enhanced material removal depth and volume, but also led to a substantial increase in friction force. This outcome was more applicable to machining methods on a wider range besides polishing.

Additionally, the damage mechanism with respect to the normal load under the presence and absence of ultrasonic vibration was concluded. In traditional scratching, the damage mechanism transited from elastic deformation to plastic deformation or possible material removal (Fig. 2). However, significant changes in the damage mechanism were not anticipated during ultrasonic-assisted scratching. Instead, material removal behavior across all loads under ultrasonic assistance demonstrated a stronger dependence on the normal load, resulting in a higher load-sensitive exponent for material removal

depth and volume.

## 5. Conclusions

Using an atomic force microscope (AFM), the single-asperity material removal behaviors of 4H-SiC against a conical diamond AFM tip were quantitatively studied under the presence and absence of ultrasonic vibration. Material removal Eq. (2) and Eq. (3) were employed to analyze the measured material removal depth and volume, respectively. The friction force was determined with the variation of normal load. Subsequently, the friction and material removal mechanisms were discussed for various normal loads, scratching speeds, and scratching distances. The main findings from this study were summarized as follows:

(1) The material removal depth and volume during ultrasonic-assisted scratching exhibited a stronger dependence on normal load compared to the traditional scratching. Although ultrasonic vibration enhanced material removal across all load levels, significant changes in the damage mechanism were not observed. In contrast, without ultrasonic vibration, the transition from elastic to plastic deformation occurred at lower normal loads, and as the load increased, SiC damage progressed from plastic deformation to wear and material removal.

(2) In the normal load range of 24 to 48 μN, ultrasonic vibration significantly increased the material removal depth and volume, while reducing or maintaining friction force. Within this range, plastic deformation became more pronounced, though elastic deformation remained influential. The increased speed and scratching distance induced by ultrasonic vibration amplified plastic deformation, leading to wear or material removal. The concurrent presence of elastic deformation and enhanced relative speed due to ultrasonic vibration contributed to the reduction in friction force.

These findings highlight the potential of ultrasonic-assisted scratching for improving material removal efficiency and reducing friction force in the processing of hard materials like 4H-SiC, particularly in industrial applications requiring precision and control.

## ACKNOWLEDGEMENT

The authors would like to thank Shenzhen Science and Technology Program (No. JSGG20220831093200001), Shenzhen Science and Technology Program (No. KQTD20170810110250357), Shenzhen Engineering Research Center for Semiconductor-specific Equipment, National Natural Science Foundation of China (No. 52105479), and Special Funds for the Cultivation of Guangdong College Students' Scientific and Technological Innovation (No. pdjh2024c10804) for their financial support.

## REFERENCES

1. Wang, Y., Dong, S., Li, X., Hong, C., and Zhang, X., "Synthesis, Properties, and Multifarious Applications of SiC Nanoparticles: A Review," Ceram. Int., Vol. 48, No. 7, pp. 8882-8913, 2022.
2. Casady, J.B., and Johnson, R.W., "Status of Silicon Carbide (SiC) as a Wide-Bandgap Semiconductor for High-Temperature Applications: A Review," Solid-State Electron., Vol. 39, No. 10, pp. 1409-1422, 1996.
3. Chen, Y., Su, H., Qian, N., He, J., Gu, J., Xu, J., and Ding, K., "Ultrasonic Vibration-Assisted Grinding of Silicon Carbide Ceramics Based on Actual Amplitude Measurement: Grinding Force and Surface Quality," Ceram. Int., Vol. 47, No. 11, pp. 15433-15441, 2021.
4. Neslen, C.L., Mitchel, W.C., and Hengehold, R.L., "Effects of Process Parameter Variations on the Removal Rate in Chemical Mechanical Polishing of 4H-SiC," J. Electron. Mater., Vol. 30, pp. 1271-1275, 2001.
5. Luo, X., Yang, W., and Qian, Y., "Fixed Abrasive Polishing: The Effect of Particle Size on the Workpiece Roughness and Sub-Surface Damage," Int. J. Adv. Manuf. Technol., Vol. 115, pp. 3021-3035, 2021.
6. Zhao, Q., Sun, Z., and Guo, B., "Material Removal Mechanism in Ultrasonic Vibration Assisted Polishing of Micro Cylindrical Surface on SiC," Int. J. Mach. Tools Manuf., Vol. 103, pp. 28-39, 2016.
7. Chen, Y., Pan, L., Yin, Z., et al., "Effects of Ultrasonic Vibration-Assisted Machining Methods on the Surface Polishing of Silicon Carbide," J. Mater. Sci., Vol. 59, pp. 7700-7715, 2024.
8. Ban, X., Zhu, J., Sun, G., Han, S., Duan, T., and Wang, N., "Molecular Simulation of Ultrasonic Assisted Diamond Grit Scratching 4H-SiC Single-Crystal," Tribol. Int., Vol. 192, pp. 109330, 2024.
9. Kim, H.J., Yoo, S.S., and Kim, D.E., "Nano-Scale Wear: A Review," Int. J. Precis. Eng. Manuf., Vol. 13, pp. 1709-1718, 2012.
10. Archard, J.F., "Contact and Rubbing of Flat Surfaces," J. Appl. Phys., Vol. 24, No. 8, pp. 981-988, 1953.
11. Bhaskaran, H., Gotsmann, B., Sebastian, A., et al., "Ultralow Nanoscale Wear Through Atom-by-Atom Attrition in Silicon-Containing Diamond-Like Carbon," Nat. Nanotechnol., Vol. 5, pp. 181-185, 2010.
12. Jacobs, T.D.B., Gotsmann, B., Lantz, M.A., et al., "On the Application of Transition State Theory to Atomic-Scale Wear," Tribol. Lett., Vol. 39, pp. 257-271, 2010.

13. Bayer, R.G., "A General Model for Sliding Wear in Electrical Contacts," Wear, Vols. 162-164, Part B, pp. 913-918, 1993.

14. Nawaz, A., Mao, W.G., Lu, C., and Shen, Y.G., "Nano-Scale Elastic-Plastic Properties and Indentation-Induced Deformation of Single Crystal 4H-SiC," J. Mech. Behav. Biomed. Mater., Vol. 66, pp. 172-180, 2017.

15. Bhushan, B., Modern Tribology Handbook, Two Volume Set, CRC Press, 2000.

16. Bhushan, B., and Ko, P.L., "Introduction to Tribology," Appl. Mech. Rev., Vol. 56, No. 1, pp. B6-B7, 2003.

17. Colaço, R., "An AFM Study of Single-Contact Abrasive Wear: The Rabinowicz Wear Equation Revisited," Wear, Vol. 267, No. 11, pp. 1772-1776, 2009.

18. Bowden, F.P., and Tabor, D., The Friction and Lubrication of Solids, Vol. 1, Oxford University Press, 2001.